agronomy

Article

Comparison of Evapotranspiration Partitioning and Dual Crop Coefficients of Direct-Seeded and Transplanted Rice in the Poyang Lake Basin, China

Bo Liu [1,*], Jiajia Hou [1], Hengjun Ge [2], Meng Liu [2], Lijie Shi [1], Cheng Li [3] and Yuanlai Cui [4]

1 College of Hydraulic Science and Engineering, Yangzhou University, Yangzhou 225009, China
2 Yangzhou Survey, Design and Research Institute Co., Ltd., Yangzhou 225002, China
3 College of Horticulture and Landscape Architecture, Yangzhou University, Yangzhou 225009, China
4 State Key Laboratory of Water Resources and Hydropower Engineering Science, Wuhan University, Wuhan 430072, China
* Correspondence: boliu@yzu.edu.cn

Abstract: Direct-seeded rice (DSR) has received much attention because of its advantages in having low labor costs compared to the traditional transplanted rice (TPR). Investigating the differences in evapotranspiration (ET) partitioning and crop coefficients (K_c) between DSR and TPR is essential in understanding how agricultural water demand is affected by crop rotation. In this study, the water fluxes of two-year (2017–2018) growing seasons were collected from a pair of eddy covariance (EC) towers for DSR and TPR in the Poyang Lake Basin, Southern China. This study aims to compare the seasonal characteristics of the ET components (evaporation, E, and transpiration, T) and dual crop coefficients (basal crop coefficient, $K_s \cdot K_{cb}$, and soil/water crop coefficient, K_e) of DSR with those of TPR. The ET values for the 2017 and 2018 growing seasons were 374 mm and 436 mm for the DSR, respectively, and 309 mm and 342 mm for the TPR. The seasonal T/ET values in 2017 and 2018 were 0.40 and 0.46 for the DSR, respectively, and 0.49 and 0.52 for the TPR, indicating that the higher ET values for the DSR can be mostly attributed to E. The DSR had overall higher K_c values than the TPR because of free water evaporation during the initial stage and a higher plant density. Our results enrich the K_c dataset for DSR and have great implications for the sustainable irrigation of the Poyang Lake Basin in the future.

Keywords: direct-seeded rice; transplanted rice; evapotranspiration partitioning; dual crop coefficient; eddy covariance

check for updates

Citation: Liu, B.; Hou, J.; Ge, H.; Liu, M.; Shi, L.; Li, C.; Cui, Y. Comparison of Evapotranspiration Partitioning and Dual Crop Coefficients of Direct-Seeded and Transplanted Rice in the Poyang Lake Basin, China. *Agronomy* **2023**, *13*, 1218. https://doi.org/10.3390/agronomy13051218

Academic Editor: Jose Manuel Gonçalves

Received: 4 April 2023
Revised: 23 April 2023
Accepted: 24 April 2023
Published: 25 April 2023

1. Introduction

Evapotranspiration (ET) is an important component of the soil–plant–atmosphere continuum (SPAC) and a key nexus in water and biochemistry cycles [1–4]. For agricultural ecosystems, ET can be partitioned into transpiration (T) through the stomata of plants and evaporation (E) from non-stomatal surfaces [5,6]. The former is closely related to plant photosynthesis [7] and is considered effective water consumption, whereas the latter is usually regarded as having no direct contribution to crop growth [8]. Rice (*Oryza sativa* L.) is a staple food for more than three billion people and plays an important role in maintaining global food security [9,10]. However, rice requires two to three times the irrigated water to produce a grain equivalent to other cereals, such as maize or wheat [11]. Therefore, estimating the ET values, and those of its components, of rice is important for better understanding the paddy field water cycle, improving water-use efficiency, and developing water-saving and high-yield field-management practices.

The crop coefficient (K_c) method proposed in the FAO-56 paper is the most widely applied method for estimating ET values [12]. Recommended K_c values are tabulated in FAO-56 and have been used for different crops in various regions. However, the K_c values are affected by field management methods, crop varieties, and climate conditions [13–15]. Many studies have demonstrated that the locally developed K_c values are lacking, so it is necessary to determine local K_c values for additional regions to enrich the K_c dataset [16,17]. Previous studies have reported various K_c values for paddy fields across different regions. Mao et al. [18] found that K_c values for the initial, mid-season, and late-season stages of paddy fields in Ningxia, Upper Yellow River Basin, China, were 1.04, 1.27, and 1.16, respectively. Choudhury and Singh. [19] indicated that the local K_c values of flooded paddy fields in India were 1.08, 1.80, and 1.41 in the initial, mid-season, and late-season stages, respectively. Lv et al. [20] reported that average K_c values were 1.10, 1.50, 1.56, and 1.28 for a flooded paddy field during the initial, crop development, mid-season, and late-season stages in southeast China, respectively, while they were 1.10, 1.34, 1.48, and 1.23 for a paddy field with controlled irrigation. In the Philippines, K_c values were 1.04, 1.11, 1.04, and 0.93 for flooded rice during the vegetative, reproductive, ripening, and fallow stages, respectively, and 0.95, 1.00, 0.97, and 0.88 for aerobic rice [21]. Kumari et al. [22] reported that actual K_c values were 1.13, 1.27, 1.23, and 0.93 for the initial, crop development, mid-season, and late-season stages, respectively, in the Indo-Gangetic plains, while Chatterjee et al. [23] found lower K_c values in eastern India (0.23–0.32, 0.42–0.52, 0.64–0.76, 0.88–0.90 for the initial, crop development, reproductive, and late-season stages). However, few studies have paid attention to the components of rice K_c: the basal crop coefficient ($K_s \cdot K_{cb}$) and soil/water evaporation coefficient (K_e) [24,25], which can further help save irrigation water and improve water-use efficiency.

The Poyang Lake Basin is one of the major rice production areas in the middle and lower reaches of the Yangtze River, Southern China. The double-rice cropping system is the conventional planting system in this area, owing to adequate thermal and sunlight conditions [26]. Typically, early rice is transplanted in late April and harvested in mid-July, and late rice is transplanted in late July and harvested in late October. However, with an increasing labor shortage, there has been a shift from the conventional cultivation of transplanted early rice (TPR) to direct-seeded early rice (DSR) in this region. Cultivating DSR can save more labor compared to transplanting rice seedlings but requires a longer growth duration [27,28]. The sowing time of early rice has been advanced to early March, which is more than one month earlier than the conventional transplanting time. This shift in planting methods from TPR to DSR may lead to changes in the ET components of early rice and influence regional water cycles and irrigation scheduling. Furthermore, the conventional K_c values for TPR may not be suitable for DSR because of the different rates of plant growth and field water conditions [29,30]. Therefore, a comparison of ET partitioning and K_c values between the TPR and DSR in the Poyang Lake Basin is important for forecasting possible changes in the crop's water demand when TPR is transformed into DSR and for identifying optimal irrigation management methods for sustainable irrigation in the future [31,32].

Given the above considerations, a pair of eddy covariance (EC) towers were set, and two-year successive water fluxes were collected at a TPR field and a DSR field in the Poyang Lake Basin, Southern China. The main aims of this study were to (1) quantify the ET, E, and T values of the TPR and DSR; (2) determine the local K_c values of TPR and DSR in the Poyang Lake Basin; (3) compare the difference in ET and K_c values between the TPR and DSR and investigate possible changes in the field water cycle when TPR was shifted to DSR.

2. Materials and Methods

2.1. Site Description

This experiment was conducted from 2017 to 2018 in the Ganfu irrigation district, Poyang Lake Basin, Jiangxi Province, China (N 28°26′27″, E 116°00′03″). This region is characterized as a subtropical, humid, and monsoonal climate. The mean annual air temperature is 18.1 ± 0.7 °C and mean annual precipitation is 1634 ± 312 mm. The soil is paddy soil with a clay loam texture and its saturated water content is 0.49 m^3 m^{-3}.

A pair of EC towers were deployed at a field with direct-seeded early rice (the DSR site) and the Jiangxi Provincial Irrigation Experiment Station with transplanted early rice (the TPR site). The straight-line distance between the two sites is less than 1.5 km. For the DSR site, the DSR was broadcast at the rate of 300 seeds m^{-2} on the wet soil surface around March 10 and harvested around July 5. The field was kept at a low standing water depth of 0–5 mm for about 45 days. Then, the typical water regime of continuous flooding (CF) irrigation was carried out to keep a 40–80 mm standing water depth. For the TPR site, the early rice seedling was first nursed in a greenhouse and then transplanted at a hill spacing of 13.3 cm × 23.3 cm with 3–4 seeds per hill (about 100 seeds m^{-2}) in late April and harvested around July 15. The TPR was irrigated following alternate wetting and drying (AWD) irrigation. The field was allowed to dry for 3–5 days before rewetting [33,34]. However, it should be noted that the field stayed flooded during the early rice season due to frequent rainfall. Thus, the irrigation method was not considered a significant factor affecting the ET values of the two paddy fields. The chemical N fertilizer was 148 kg N ha^{-1} for the early rice at the DSR site, and 160 kg N ha^{-1} for the early rice at the TPR site.

2.2. Field Measurements

The EC system at the DSR site was equipped with a sonic anemometer (WindMaster Pro, Gill Instruments Inc., Poole, UK), an open path CO_2/H_2O gas analyzer (LI-7500A, Li-COR Biosciences Inc., Lincoln, NE, USA), and a data logger (LI-7550, Li-COR Biosciences Inc., Lincoln, NE, USA) to record raw data from the EC system. As for the TPR site, the CO_2/H_2O gas analyzer and data logger were the same as those at the DSR site, while the R3-50 (Gill Instruments Inc., Poole, UK) was used to monitor high-frequency wind speed in 3D. All sensors for the two sites were installed at a height of 2.5 m above ground level. Meteorological sensors at each site included a combined humidity and temperature sensor (HMP155, Vaisala Inc., Vantaa, Finland), a net radiometer (NR Lite 2, Kipp&Zonen Inc., Delft, Netherlands), and a photosynthetically active radiation sensor (LI-190SB, Li-COR Biosciences Inc., Lincoln, NE, USA) installed at a height of 3 m, as well as three soil heat flux plates (HFP01, Hukseflux Inc., Delft, Netherlands) and three combined soil moisture and temperature sensors (ML2x, Delta-T Devices Inc., Cambridge, UK) buried at a depth of 5 cm and a tipping bucket rain gauge (TR-525M, Texas Electronics Inc., Dallas, TX, USA). The meteorological data from the two sites were used for mutual gap-filling to produce the complete annual data series [26].

2.3. Data Processing, Gap Filling and Flux Partitioning

High frequency (10 Hz) flux raw data were processed using the EddyPro software following standard routines. Correction practices included coordinate rotation via double rotation [35], correction for density fluctuations (WPL-correction) [36], spectral correction [37], and spike detection. After corrections, the latent heat (LE), sensible heat (H), and net ecosystem exchange (NEE) of CO_2 fluxes over 30-min intervals were collected as output. The output data for periods flagged as low quality by EddyPro as well as periods where there was rainfall, instrument malfunction, or human disturbance were removed. Flux data were also removed when friction velocity (u*) was less than 0.15 m s^{-1} [33,34]. The energy fluxes (LE and H) were gap-filled using the REddyProc tool from the Max Planck Institute for Biogeochemistry [38], while the CO_2 fluxes were gap-filled and partitioned using the non-linear regression (NLR) method [39,40]. The NLR method was selected based on the assumption that the nighttime net ecosystem exchange (NEE) of CO_2 fluxes was equal to ecosystem respiration (R_{eco}) due to the absence of plant photosynthesis, while daytime NEE can be described as the difference between R_{eco} and gross primary productivity (GPP):

$$NEE = \begin{cases} R_{eco} & \text{nighttime} \\ R_{eco} - GPP & \text{daytime} \end{cases} \tag{1}$$

Details of the gap-filling and partitioning procedure for the CO_2 fluxes can be found in Liu et al. [26].

The underlying water-use efficiency (uWUE) method [41] was applied to partition ET into E and T. This method has been applied across various croplands [42–45] as well as the study area [46] and can provide reliable ET components.

The uWUE method relies on the estimatation of two uWUE variants, the potential uWUE (uWUEp), and the apparent uWUE (uWUEa), which can be defined as:

$$uWUE_p = \frac{GPP \cdot VPD^{0.5}}{T} \tag{2}$$

$$uWUE_a = \frac{GPP \cdot VPD^{0.5}}{ET} \tag{3}$$

where VPD is the vapor pressure deficit. By assuming the ecosystem T is equal to ET when vegetation coverage is high, the $uWUE_p$ can be calculated using the 95th percentile regression between half-hour $GPP \cdot VPD^{0.5}$ and ET from the whole year. The value of $uWUE_a$ is estimated using the linear regression slope from a moving window depending on the study period. T/ET is then estimated as:

$$\frac{T}{ET} = \frac{uWUE_a}{uWUE_p} \tag{4}$$

2.4. Calculation of Parameters

The daily ET_0 was calculated following the Penman-Monteith equation recommended by FAO-56 [12]. This method has been considered the standard method of ET_0 estimation, and many studies have demonstrated its accuracy and universality in different climate zones [47,48]. The FAO-56 PM equation is described as follows:

$$ET_0 = \frac{0.408\Delta(R_n - G) + \gamma \frac{900}{T_{mean}+273} u_2(e_s - e_a)}{\Delta + \gamma(1 + 0.34u_2)} \tag{5}$$

where R_n is the surface net radiation (MJ m^{-2} d^{-1}), G is the soil heat flux (MJ m^{-2} d^{-1}), T_{mean} is the mean air temperature (°C), i.e., T_{mean} = (T_{max} + T_{min})/2, u_2 is the wind speed at 2 m height (m s^{-1}), e_s is the saturation vapor pressure (kPa), e_a is the actual vapor pressure (kPa), Δ is the slope of the saturation vapor pressure curve (kPa °C^{-1}), and γ is the psychometric constant (kPa °C^{-1}).

The daily K_c can be estimated as the ratio of daily ET and ET_0 [13,15–17]:

$$K_c = \frac{ET}{ET_0} \tag{6}$$

As recommended by the FAO-56, K_c can be split into two coefficients that describe soil/water evaporation (K_e) and plant transpiration ($K_s \cdot K_{cb}$):

$$K_c = K_s \cdot K_{cb} + K_e \tag{7}$$

where K_s is the stress coefficient, $K_s \cdot K_{cb}$ is the basal crop coefficient, and K_e is soil/water evaporation. E and T can be used to partition the K_c into $K_s \cdot K_{cb}$ and K_e as follows:

$$K_e = \frac{E}{ET_0} \tag{8}$$

$$K_s \cdot K_{cb} = \frac{T}{ET_0} \tag{9}$$

To reveal the phenology controls of the paddy field on K_c, the canopy conductance (G_c) was calculated by inverting the Penman-Monteith formula:

$$G_c = \frac{\gamma \cdot ET \cdot G_a}{\Delta(R_n - G) + \rho_a \cdot c_p \cdot VPD \cdot G_a - ET(\Delta + \gamma)} \quad (10)$$

where γ is the psychometric constant (kPa °C^{-1}), G_a is the aerodynamic conductance (m s^{-1}), ρ_a is the air density (kg m^{-3}), Δ is the slope of the saturation vapor pressure curve (kPa °C^{-1}), c_p is the air heat capacity at constant pressure (J kg^{-1} °C^{-1}), and VPD is the saturation vapor pressure deficit (kPa).

The G_a was estimated using the following equation [49]:

$$G_a = \frac{K^2 u_z}{\ln \frac{Z_m - d}{Z_{om}} \cdot \ln \frac{Z_h - d}{Z_{oh}}} \quad (11)$$

where K is the von Karman's constant, K = 0.41, Z_m and Z_h were the heights of measured wind speed and relative humidity, respectively (m), d is the zero plane displacement height (m), d = 2/3 h (h is plant height, m), Z_{om} is the roughness length governing momentum transfer (m) Z_{om} = 0.123 h, and Z_{oh} is the roughness length governing the transfer of heat and vapor (m), Z_{oh} = 0.1 Z_{om}.

2.5. Statistical Analysis

The performance of the 'ET_0-K_c' method was evaluated using three statistical indices, including the mean absolute error (MAE), the mean square error (RMSE), and the coefficient of determination (R^2). The three indices are described as follows:

$$MAE = \frac{\sum_{i=1}^{m} |S_i - M_i|}{m} \quad (12)$$

$$RMSE = \sqrt{\frac{\sum_{i=1}^{m} (S_i - M_i)^2}{m}} \quad (13)$$

$$R^2 = \frac{\sum_{i=1}^{m} (S_i - M_i)^2}{\sum_{i=1}^{m} (M_i - \overline{M})^2} \quad (14)$$

where m is the number of measurements, S_i and M_i are simulated and measured values, respectively, and $\overline{M}$ is the mean of measued values.

3. Results

3.1. Meteorological Conditions and Energy Balance Closure

Seasonal variations and stage-wise average meteorological factors during the DSR and TPR seasons are shown in Figure 1 and Table 1. The seasonal variations of R_n and T_a showed overall increasing trends despite large fluctuations due to rainy or cloudy weather conditions. The seasonal average R_n was 6.4 and 7.9 MJ m^{-2} d^{-1} for the DSR, and 8.0 and 9.2 MJ m^{-2} d^{-1} (Table 1). for the TPR in 2017 and 2018, respectively. The seasonal average T_a was 20.9 and 23.0 °C for the DSR, and 24.9 and 27.2 °C for the TPR in 2017 and 2018, respectively. In addition, Table 1 showed that the R_n and T_a of different growth stages for the DSR were generally lower than those for the TPR. The R_n and T_a in 2018 were higher than those in 2017 for both the DSR and TPR, providing better light and thermal conditions for rice growth. Similar to the seasonal variation of T_a, the pattern of VPD also showed a general increasing trend from April to July. Values of W_s showed no clear seasonal pattern. Meanwhile, there was no obvious difference in the seasonal average W_s between the DSR and TPR. The stage-wise W_s ranged from 0.8 to 2.2 m s^{-1} for the DSR and 0.7 to 1.7 m s^{-1} for the TPR during the two-year growing seasons. The G_c presented higher values during the initial stages of the DSR, which may be explained by near water surface evaporation. After that, the G_c of DSR showed similar seasonal variations to that of the TPR. The G_c gradually increased with the growth of rice plants and then decreased during canopy senescence.

Table 1. Meteorological factors including net radiation (R_n), air temperature (T_a), vapor pressure deficit (VPD), wind speed (W_s), precipitation (P), and actual evapotranspiration (ET), evaporation (E) and transpiration (T), of direct-seeded rice (DSR) and transplanted rice (TPR) in 2017 and 2018.

Year	Rice	Stages	Days (d)	R_n (MJ m^{-2} d^{-1})	T_a (°C)	VPD (kPa)	W_s (m s^{-1})	P (mm)	ET (mm)	E (mm)	T (mm)	T/ET
2017	DSR	Ini *	32	4.3	14.4	0.38	2.0	327	66	60	6	0.09
		Dev	27	7.6	20.9	0.78	1.6	97	96	82	14	0.15
		Mid	48	7.7	24.7	0.74	1.4	231	182	67	115	0.63
		Lat	11	5.2	25.3	0.39	0.8	207	30	16	14	0.48
		Seasonal	118	6.4	20.9	0.61	1.4	861	374	225	149	0.40
	TPR	Ini	10	7.7	20.4	0.75	1.7	65	33	28	5	0.17
		Dev	15	9.3	23.5	0.95	1.3	69	60	39	21	0.35
		Mid	39	6.7	24.9	0.65	1.5	244	123	46	77	0.62
		Lat	21	9.6	28.1	0.78	0.7	165	93	44	49	0.53
		Seasonal	85	8.0	24.9	0.74	1.3	542	309	157	152	0.49
2018	DSR	Ini	29	6.0	16.4	0.55	1.5	116	76	68	8	0.11
		Dev	29	7.3	20.2	0.71	1.6	244	113	71	41	0.37
		Mid	46	8.6	26.4	0.85	1.5	332	198	70	128	0.65
		Lat	12	11.3	30.0	0.82	2.2	24	49	26	22	0.46
		Seasonal	116	7.9	23	0.75	1.6	715	436	235	201	0.46
	TSR	Ini	8	7.3	23	0.64	1.6	45	17	14	3	0.18
		Dev	19	10.4	25.8	0.87	1.6	79	87	57	30	0.34
		Mid	37	8.3	27.1	0.87	1.6	221	147	49	98	0.67
		Lat	20	10.5	30.3	1.01	1.7	107	91	45	46	0.51
		Seasonal	84	9.2	27.2	0.89	1.6	451	342	165	177	0.52

* Ini is short for initial stage; Dev is short for crop development stage; Mid is short for mid-season stage; Lat is short for late-season stage.

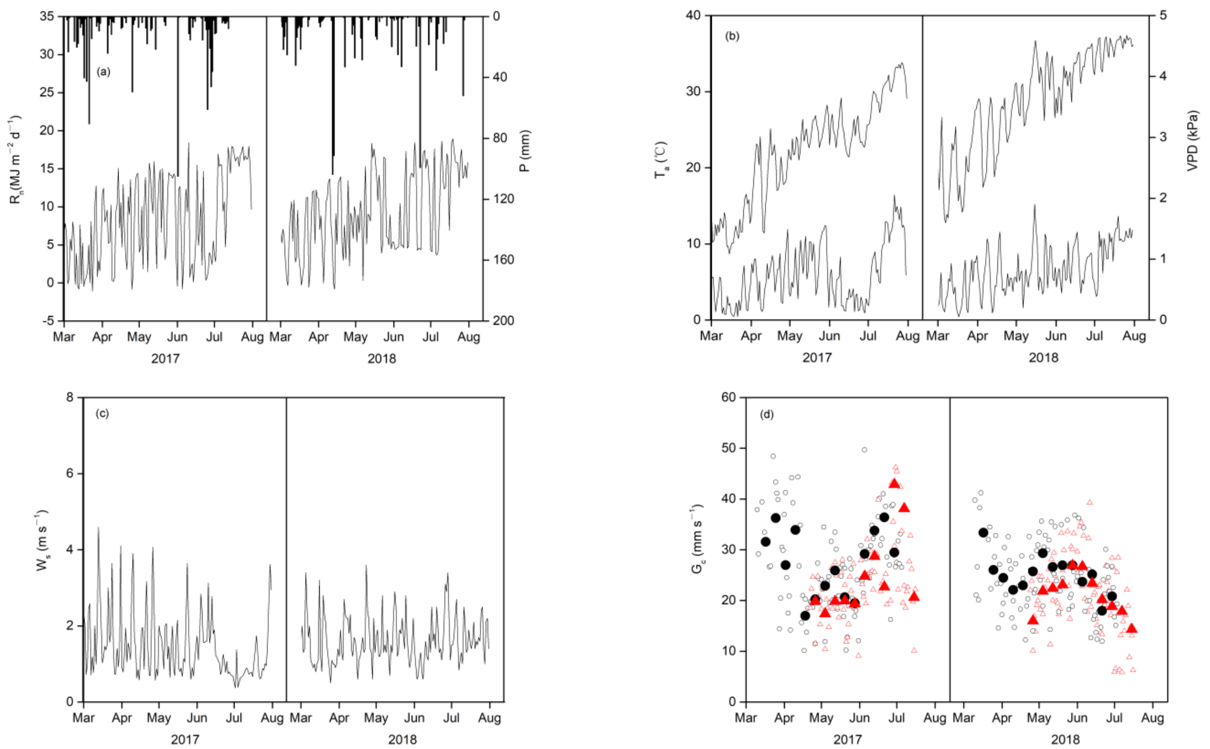

Figure 1. Seasonal variation of main meteorological factors during the rice growth season in 2017 and 2018. (**a**) Net radiation (R_n) and precipitation (P), (**b**) air temperature (T_a) and vapor pressure deficit (VPD), and (**c**) wind speed (W_s) and (**d**) canopy conductance (G_c). The hollow black dots and red triangles denote daily G_c of DSR and TPR, respectively. The solid black dots and red triangles denote the 8-day average G_c of DSR and TPR, respectively.

Figure 2 shows a comparison between the available energy (R_n-G) and turbulence energy (LE + H) of the DSR and TPR in 2017 and 2018. Slopes were 0.77 for the DSR and 0.68 for the TPR in 2017, and 0.75 for the DSR and 0.63 for the TPR in 2018. Intercepts ranged from 33.12 to 41.15 W m^{-2} for the two sites. The degree of the energy balance closure was within the results of FLUXNET [50] and ChinaFlux [51], indicating that the paired EC system in our study provides a reliable measurement of turbulence fluxes for DSR and TPR fields. However, a comparison of the evapotranspiration partitioning and dual crop coefficients requires the energy balance to be closed. Thus, we adopted the Bowen ratio-closure method proposed by Wohlfahrt et al. [52] to overcome the energy imbalance.

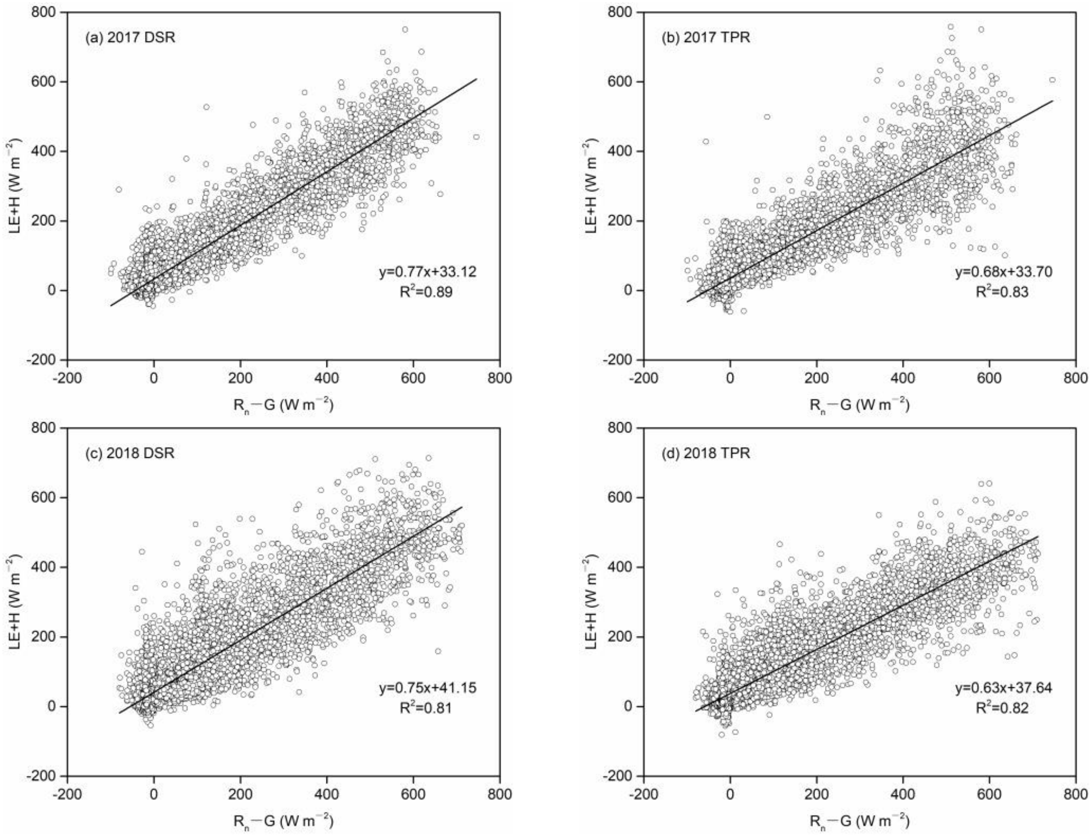

Figure 2. Comparison between available energy (R_n-G) and turbulent energy fluxes (H + LE) for (**a**) direct-seeded rice (DSR) and (**b**) transplanted rice (TPR) in 2017, and (**c**) direct-seeded rice (DSR) and (**d**) transplanted rice (TPR) in 2018. The solid lines are the linear regression fit.

3.2. Seasonal Variation in Evapotranspiration, Evaporation, and Transpiration

Figure 3 shows the seasonal variation in daily ET, E, and T values during growing seasons for the DSR and TPR in 2017 and 2018. The general patterns of variation in daily ET, E, and T were similar over the two years. Values of ET showed an overall increasing trend for both DSR and TPR, which was consistent with the seasonal variations of R_n. Meanwhile, ET also showed frequent fluctuations as a result of rainy and cloudy days. During the late-season stage, ET on sunny days still stayed relatively high because of climbing radiation and temperatures. Values of E and T showed different seasonal variations during the growing season. During the initial stage, the daily T stayed at a low value and E was the main component of ET. At this stage, the T/ET was 0.09 and 0.11 for the DSR in 2017 and 2018, respectively, which was lower than that for the TPR (0.17 in 2017 and 0.18 in 2018, Table 1). The difference in T/ET for the DSR and TPR during the initial stage was closely related to the planting method. For the DSR, the rice seeds grew slowly after broadcast since the temperature in March and early April was still low. Thus, the T was fairly low, ranging from 0.06 to 0.60 mm d^{-1} because of the small and short rice seedlings. However, the TPR seedlings were already raised in greenhouse seedbeds for about one month, resulting in relatively larger rice seedlings and larger T (0.12–1.11 mm d^{-1}) during the initial stage. With the growth of rice seedlings for both the DSR and TPR, T gradually increased and reached its peak during the mid-season stage. Simultaneously, E first increased due to the increasing solar radiation and then decreased as the rice canopy started to close. The mid-season T/ET was 0.63 and 0.65 for DSR, and 0.62 and 0.67 for TPR in 2017 and 2018, respectively. As the rice matured, its leaves became yellow, which resulted in a decreasing proportion of T in ET. The total growing season ET for the DSR was 374 mm and 436 mm, which was 65 mm and 94 mm higher than that for the TPR in 2017 and 2018, respectively. The seasonal T/ET for the DSR and TPR were 0.40 and 0.49 in 2017, and 0.46 and 0.52 in 2018, respectively, indicating the higher ET for DSR was mostly attributed to field water evaporation (E).

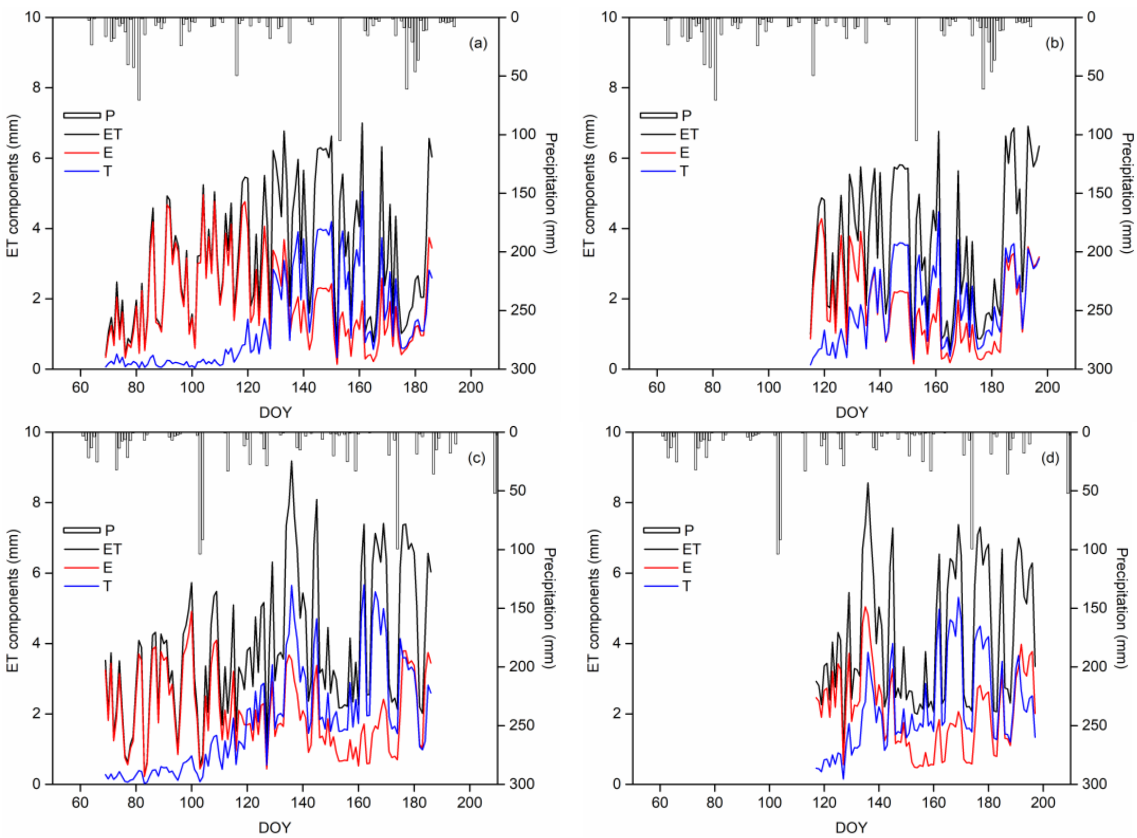

Figure 3. Seasonal variation in evapotranspiration (ET), transpiration (T), and evaporation (E) of (**a**) direct-seeded rice (DSR) in 2017, (**b**) transplanted rice (TPR) in 2017, (**c**) direct-seeded rice (DSR) in 2018, and (**d**) transplanted rice (TPR) in 2018. DOY is day of the year.

3.3. Single and Dual Crop Coefficients

Figure 4 shows the daily K_c values and local developed K_c curves for the DSR and TPR in 2017 and 2018. The K_c in the initial stage for the DSR in 2017 and 2018 were both 1.20, which was higher than that for TPR (1.14 in 2017 and 1.11 in 2018). With the growth of rice crops, daily K_c gradually increased and stayed at relatively high values during the mid-season stage. The average K_c values during the mid-season stage were 1.38 and 1.33 for the DSR, and 1.29 and 1.27 for the TPR in 2017 and 2018, respectively. The K_c values then gradually decreased during the late-season stage with the senescence of rice. The lowest value of K_c is closely related to the duration of the late-season stage. The longer the late-season stage, the more senescent the rice leaves and the drier the field soil, thus leading to a lower K_c at the end of the late-season stage.

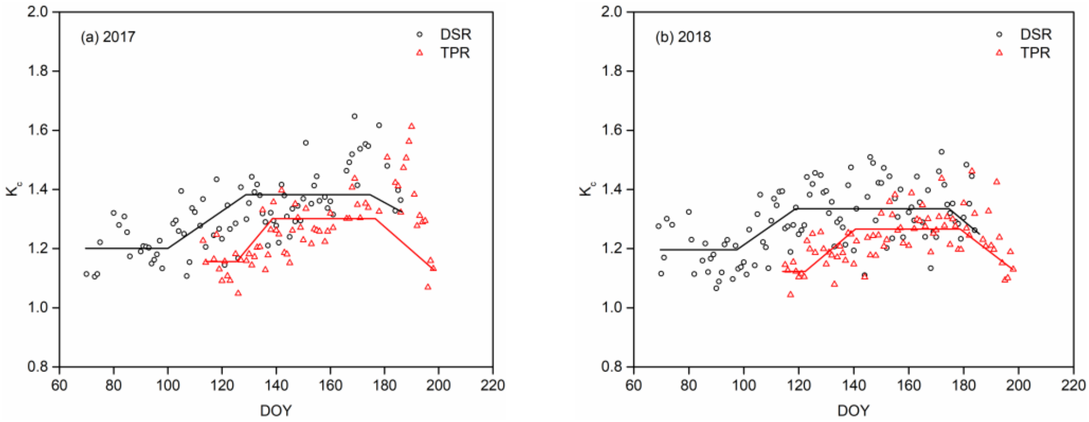

Figure 4. Daily crop coefficient (K_c) and locally developed K_c curves for direct-seeded rice (DSR) and transplanted rice (TPR) in (**a**) 2017 and (**b**) 2018. DOY is the day of the year.

Figure 5 shows the seasonal variation in the measured ET (ET_m) and simulated ET (ET_s) using the 'ET_0-K_c' method for the DSR and TPR in 2017 and 2018, as well as the linear regression analysis between ET_m and ET_s. The results showed that ET_s was highly correlated with ET_m. The slope of the fitted linear regression between ET_s and ET_m was 0.89 for the DSR and 0.96 for the TPR in 2017, and 0.91 and 0.96, respectively in 2018. The root mean square errors (RMSE) were 0.270 mm d^{-1} for the DSR and 0.407 mm d^{-1} for the TPR in 2017, and 0.349 mm d^{-1} for the DSR and 0.284 mm d^{-1} for the TPR in 2018. The coefficients of determination (R^2) for the fitted linear regression were high, ranging from 0.977 to 0.989. These results indicate that the 'ET_0-K_c' method can provide an accurate simulation of ET. Therefore, the locally developed K_c curve can be used to estimate ET and guide irrigation scheduling for both DSR and TPR.

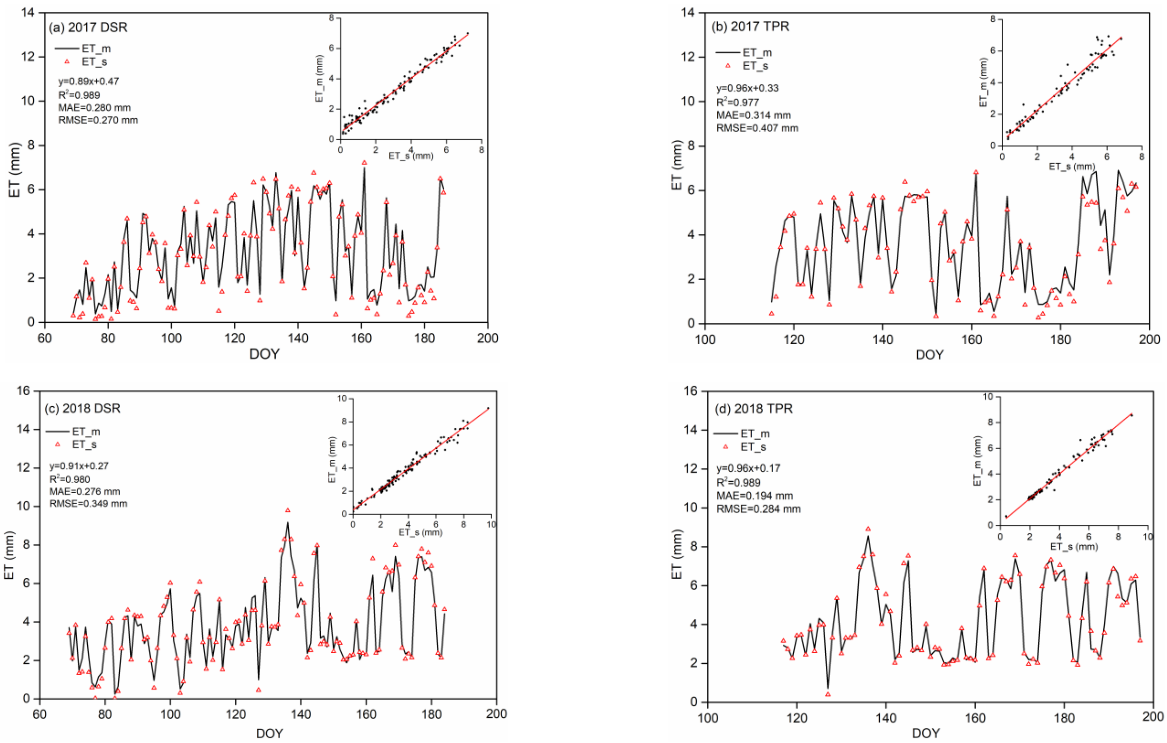

Figure 5. Comparison between measured evapotranspiration (ET_m) and simulated evapotranspiration (ET_s) for (**a**) direct-seeded rice (DSR) ans (**b**) transplanted rice (TPR) in 2017, and (**c**) direct-seeded rice (DSR) and (**d**) transplanted rice (TPR) in 2018. The red, solid lines are the linear regression fit.

Figure 6 shows the daily basal crop coefficient ($K_s \cdot K_{cb}$) and soil/water evaporation coefficient (K_e) of the DSR and TPR in 2017 and 2018. For the DSR, the $K_s \cdot K_{cb}$ remained at low values during the initial stage since the T was low in March and early April. Then, the $K_s \cdot K_{cb}$ rapidly increased and reached its peak values of 1.08 (DOY 167) in 2017 and 1.05 (DOY 165) in 2018. During the mid-season stage, the average $K_s \cdot K_{cb}$ values in 2017 and 2018 were both 0.87. Then, the $K_s \cdot K_{cb}$ gradually decreased to about 0.6 with the senescence of paddy rice. For the TPR, the variation of $K_s \cdot K_{cb}$ during the growth season was similar to that of the DSR, except for the initial stage. At the initial stage, the $K_s \cdot K_{cb}$ of the TPR increased rapidly after the rice seedlings were transplanted. Unlike the DSR, the TPR was already nursed and could spring up after the rice seedlings recovered from the shock of uprooting. This recovery period is also known as the regreening stage or transplanting stage, which usually lasts about seven days in the study area. However, despite the rapid increase in the $K_s \cdot K_{cb}$ of the TPR, the $K_s \cdot K_{cb}$ remained lower than that for the DSR until near DOY 170, when the $K_s \cdot K_{cb}$ of both the DSR and TPR reached their peaks. On a seasonal basis, the $K_s \cdot K_{cb}$ of the DSR was 0.51 in 2017 and 0.58 in 2018, which was slightly lower than that of the TPR (0.64 in 2017 and 0.65 in 2018). This is consistent with the results of T/ET for the DSR and TPR. The K_e showed opposite variation trends with $K_s \cdot K_{cb}$ in the growing season. The average K_e at the initial, crop development, mid-season, and late-season season stages were 1.09, 1.10, 0.51, and 0.74 in 2017, and 1.07, 0.83, 0.46, and 0.74 in 2018 for the DSR (Table 2), which were slightly higher than the corresponding values of K_e for the TPR, indicating more evaporation loss for the DSR.

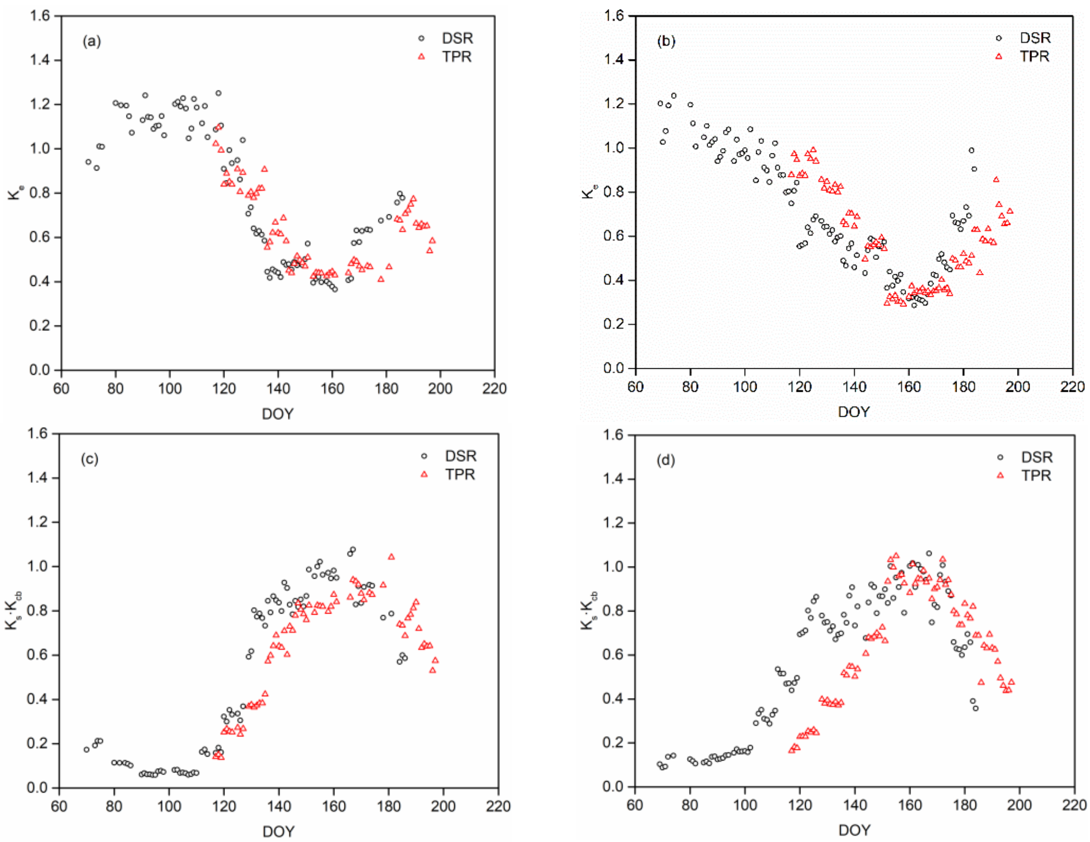

Figure 6. Evaporation coefficients (K_e) and basal crop coefficients ($K_s \cdot K_{cb}$) for direct-seeded rice (DSR) and transplanted rice (TPR). (**a**) K_e in 2017, (**b**) K_e in 2018, (**c**) $K_s \cdot K_{cb}$ in 2017, and (**d**) $K_s \cdot K_{cb}$ in 2018. DOY is the day of the year.

Table 2. Stage-wise local crop coefficients (K_c), evaporation coefficients (K_e), and basal crop coefficients ($K_s \cdot K_{cb}$) for direct-seeded rice (DSR) and transplanted rice (TPR) in 2017 and 2018.

Year	Rice	Stages	K_c	K_e	$K_s \cdot K_{cb}$
2017	DSR	Ini	1.20	1.09	0.11
		Dev	1.28	1.10	0.18
		Mid	1.38	0.51	0.87
		Lat	1.40	0.74	0.66
		Seasonal	1.32	0.81	0.51
	TPR	Ini	1.14	0.93	0.21
		Dev	1.18	0.78	0.40
		Mid	1.29	0.49	0.80
		Lat	1.37	0.64	0.73
		Seasonal	1.27	0.63	0.64
2018	DSR	Ini	1.20	1.07	0.13
		Dev	1.30	0.83	0.47
		Mid	1.33	0.46	0.87
		Lat	1.32	0.74	0.58
		Seasonal	1.29	0.71	0.58
	TSR	Ini	1.11	0.91	0.20
		Dev	1.21	0.81	0.40
		Mid	1.27	0.40	0.87
		Lat	1.24	0.61	0.63
		Seasonal	1.23	0.59	0.65

4. Discussion

4.1. Comparison of Evapotranspiration Partitioning for Direct-Seeded and Transplanted Rice

DSR has been regarded as a promising technology to save irrigation water [14,28,53]. One of the reasons that DSR could save irrigation water is that it does not have a so-called 'field-ponding period'. For the traditional TPR, rice seeds are nursed at seedbeds for about three to four weeks before being transplanted to the field [26]. In the meantime, the field is flooded for a few days to soak the soil of the plow layer. This field-ponding period requires a large amount of irrigation water, of which most is lost through seepage or percolation [54,55]. On the contrary, rice seeds are directly seeded in the field for DSR and requires no such ponding water. Another reason is the difference in amount of water required during the initial stage between DSR and TPR. According to the field water condition at seeding, DSR can be classified as dry-seeded, wet-seeded, or water-seeded rice. Dry-seeded and wet-seeded rice are usually procured in rainfed areas and not irrigated during the initial stage [53,56]. While water-seeded rice keeps the standing water depth at low levels during the initial stage, DSR provides an opportunity to fully use the early season rainfall and hence save irrigation water. In this study, rainfall during the initial stage was 327 and 116 mm in 2017 and 2018, respectively. This met a large portion of the water requirements for the DSR. An experiment in northwest India found that dry-seeded rice can save 35% to 57% of irrigation water [57,58]. Kumar et al. [59] compared the water balance of TPR and DSR with different irrigation regimes based on soil matric potential levels. Their results indicated that DSR can reduce from 14.7% to 60.8% more irrigation water than TPR. A case study in central China showed that dry-seeded rice used 15.3% less water than TPR [60].

However, if we consider water loss on a regional scale, the actual water loss from paddy fields is attributed to evapotranspiration (ET). The percolation and drainage water of paddy fields eventually recharges the groundwater [61,62] or can be re-used in the form of return flow [63,64]. In this study, the DSR evaporated between 25.1% and 28.2% more water than the TPR during the growing season. The seasonal T of the DSR was the same as that of the TPR in 2017, and only 29 mm higher in 2018, indicating the difference in ET between the DSR and TPR can be mainly attributed to E. Despite the larger ET loss, the higher plant density and avoidance of the shock of uprooting resulted in more biomass and gross primary production (GPP) under water-ample conditions [26,65,66]. This raised the question of whether or not the extra evaporated water produced proportional GPP. Table 3 compares the ecosystem water-use efficiency (WUE = GPP/ET) and transpiration-based WUE (tWUE = GPP/T) of the DSR and TPR. As we can see, the WUE was 1.59 and 1.73 g C kg^{-1} H_2O for the DSR in 2017 and 2018, respectively. The WUE for the DSR was higher than the values observed at the paddy field in the Liaohe Delta, Northeast China (1.35–1.36 g C kg^{-1} H_2O) [67] and comparable to that of Southern Brazil (1.51–1.75 g C kg^{-1} H_2O in 2010–2015) [68] but lower than that of the TPR in this study (1.87 and 1.90 g C kg^{-1} H_2O in 2017 and 2018). However, if we exclude the E, which is ineffective for GPP, the tWUE shows little difference between the DSR and TPR in both years. Our results indicated that the DSR and TPR had similar tWUE, and the lower WUE for the DSR was mainly caused by less effective evaporation.

Table 3. Seasonal ecosystem water-use efficiency and transpiration-based water-use efficiency of direct seeded rice and transplanted rice in 2017 and 2018.

Year	Rice	ET (mm)	T (mm)	GPP (g C m^{-2})	WUE (g C kg^{-1} H_2O)	tWUE (g C kg^{-1} H_2O)
2017	DSR	374	149	593	1.59	3.98
	TPR	309	152	579	1.87	3.81
2018	DSR	436	201	754	1.73	3.75
	TSR	342	177	651	1.90	3.68

4.2. Variation in Crop Coefficients of Direct-Seeded and Transplanted Rice

The K_c values of rice have been estimated across various regions [20–22,69–72], while only several studies have reported K_c values of DSR. Compared to TPR, different methods of water management during the early-season stage may result in differences in K_c values [30,73]. Dry-seeded rice usually displays a lower K_c value during the early-season stage because of more aerobic soil conditions. Alberto et al. [24] reported that the K_c of dry-seeded rice during the initial stage was 0.81 and 0.84 in a two-year study period in the Philippines. Choudhury et al. [74] estimated the K_c values of dry-seeded rice in the conventional flat land in Indo-Gangetic plains, India, and the results indicated that the K_c values of the dry-seeded rice was 0.61 during the initial stage. For water/wet-seeded rice, K_c values during the initial stage can be much larger. Linquist et al. [29] showed the K_c values of water-seeded rice and dry-seeded rice with more than twice-flushed irrigation (soil surface was not often dry) ranged from 1.17 to 1.24 during the first 30 days in the Sacramento Valley of California, USA. Additionally, the K_c values during the initial stage were also found to be larger than those of the mid-season stage because of the higher evaporation of the flooded water surface. Another study by Montazar et al. [75] also indicated that the K_c value during the initial stage was highest across the whole growing season for flooded DSR in California.

In this study, the K_c values of the DSR during the initial stage were 1.20 in both 2017 and 2018, which was higher than that of the TPR and comparable with the results of Linquist et al. [29]. However, our study presented higher K_c values for the mid-season stage than the initial stage for the flooded DSR, which may be explained by the higher plant density [26]. The K_c values tended to increase with increasing plant density [13,76–78]. Choudhury et al. [74] also indicated that dry-seeded rice with narrower spacing had higher mid-season K_c values. Higher plant density resulted in higher canopy conductance (G_c) and may have increased the K_c, as many studies have indicated that K_c values are closely related to G_c values [45,79]. Figure 7 displays the correlation between K_c and G_c values over the two study years. To avoid data instability caused by rainy and cloudy days, the eight-day average G_c and K_c values were used. As we can see, the relationships between G_c and K_c values are significant (R^2 = 0.682). The K_c values of the DSR being higher than those of the TPR is closely related to the higher G_c value (Figure 1d) caused by its dense cultivation. This relationship was not identified in the data during the initial stage of DSR cultivation, which may be caused by the uncertainty of the Penman-Monteith model when the field is near the water surface.

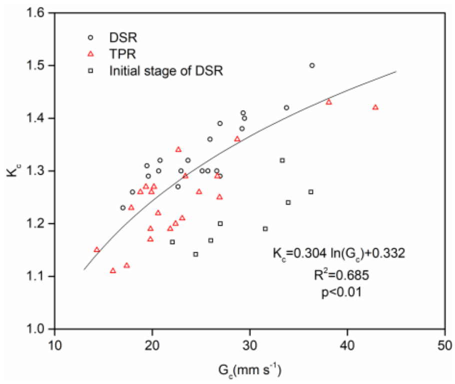

Figure 7. Relationship between 8-day crop coefficients (K_c) and canopy conductance (G_c) of direct seeded rice (DSR) and transplanted rice (TPR). The solid line is fitted curve.

The partitioning of K_c indicated that the higher K_c values of the DSR for the mid-season stage was mostly caused by $K_s{\cdot}K_{cb}$ (Table 2). This result further confirms our hypothesis that the higher K_c value of the DSR during the mid-season stage is due to its higher plant density. However, different from the previous results [78,79], the K_e value of the DSR during the mid-season stage was not lower than that of the TPR. This is because the DSR and TPR had different growing seasons as well as growth stages. If we compare contemporaneous K_c values, it can be seen that the K_e value for the DSR is lower than that of the TPR until the DSR begins to senesce (Figure 5). Given the above discussion, we suggest that researchers should consider plant density or row spacing in describing field management methods involving K_c research. In this study, the two-year average mid-season $K_s{\cdot}K_{cb}$ was 0.87 and 0.81 for the DSR and TPR, respectively. While numerous studies have estimated K_c values of paddy fields, the $K_s{\cdot}K_{cb}$ is not often reported. Alberto et al. [24] indicated the $K_s{\cdot}K_{cb}$ during the mid-season stage was 0.95 for a dry-seeded paddy field with sprinkler irrigation in the Philippines. Vories et al. [25] reported the $K_s{\cdot}K_{cb}$ for an aerobic paddy field in Missouri, USA, was 1.18 during the mid-season stage. Our results of $K_s{\cdot}K_{cb}$ values are lower than the above two studies, which may be related to the lower T/ET. Compared to the dry-seeded rice with sprinkler irrigation in the Philippines and aerobic rice in Missouri, USA, the paddy field in our study was flooded and therefore lead to a higher proportion of E in ET.

It should be noted that our results are based on measurements of the EC method, while many other methods, such as the lysimeter (weighing or non-weighing), water balance, sap flow, etc., are also used to derive crop K_c values [22]. The differences caused by measurement methods are worth attention. The EC method has advantages in continuous, long-term, undisturbed, and large-scale measurements [33,34] and has been greatly promoted for obtaining crop K_c values in recent years. However, this method also suffers from many problems, such as an energy imbalance and data gaps. Choosing appropriate energy closures and gap-filling methods is essential in acquiring accurate K_c values. Moreover, since most of paddy fields are located in humid regions, where more rainy days may occur during the rice growing season, missing data may be massive compared to those of semi-arid or arid regions. Therefore, the uncertainty caused by gap-filling methods should be evaluated in the future for accurate rice K_c values when using the EC technique.

5. Conclusions

Based on two growing seasons of water fluxes measured with paired EC towers deployed at two neighboring paddy fields in the Poyang Lake Basin, Southern China, this study compared the differences in ET, its components (E and T), and crop coefficients between direct seeded rice (DSR) and the transplanted rice (TPR). The seasonal ET of the DSR was 374 mm in 2017 and 436 mm in 2018, which was 65 mm and 94 mm higher than that of the TPR. The partitioning of ET into E and T showed that the higher ET of the DSR is mostly attributed to E, indicating that more ineffective evaporation was lost for the DSR. The K_c values of the DSR were 1.20, 1.28, 1.38, and 1.40 in 2017 and 1.20, 1.30, 1.33, and 1.32 in 2018 during the initial, crop development, mid-season, and late-season stages, respectively. The corresponding K_c values for the TPR were generally lower. The intense water evaporation during the initial stage and the higher plant density may be the main reasons for the higher K_c of the DSR. Our study implies that the transformation of rice cultivation from TPR to DSR may result in more water loss in the future. In addition, the DSR can save the field ponding water but requires more irrigation water during the mid-season stage. Under the background of climate warming, the frequency of drought may increase during the mid-season stage and cause a higher risk of irrigation water shortage with DSR cultivation. This study is important for better understanding agricultural water use in rice-dominated regions as affected by human activities and making reasonable irrigation schedules in the future.

Author Contributions: Conceptualization, B.L. and Y.C.; data curation, J.H., M.L. and L.S.; formal analysis, H.G. and C.L.; methodology, L.S.; supervision, B.L.; validation, M.L.; writing—original draft, B.L.; writing—review and editing, B.L. All authors have read and agreed to the published version of the manuscript.

Funding: This research was financially supported by the NSFC-MWR-CTGC Joint Yangtze River Water Science Research Project (No. U2040213) and the Natural Science Foundation of the Jiangsu Higher Education Institutions of China (21KJB210021).

Data Availability Statement: Not applicable.

Acknowledgments: We also would like to thank the editor, and the anonymous reviewers, for their insightful comments and constructive suggestions.

Conflicts of Interest: The authors declare no conflict of interest.

References

1. Ma, N.; Zhang, Y.; Guo, Y.; Gao, H.; Zhang, H.; Wang, Y. Environmental and biophysical controls on the evapotranspiration over the highest alpine steppe. *J. Hydrol.* **2015**, *529*, 980–992. [CrossRef]
2. Qiu, R.; Liu, C.; Cui, N.; Wu, Y.; Wang, Z.; Li, G. Evapotranspiration estimation using a modified Priestley-Taylor model in a rice-wheat rotation system. *Agric. Water Manag.* **2019**, *224*, 105755. [CrossRef]
3. Djaman, K.; Koudahe, K.; Mohammed, A.T. Dynamics of Crop Evapotranspiration of Four Major Crops on a Large Commercial Farm: Case of the Navajo Agricultural Products Industry, New Mexico, USA. *Agronomy* **2022**, *12*, 2629. [CrossRef]
4. Sun, X.; Wilcox, B.P.; Zou, C.B. Evapotranspiration partitioning in dryland ecosystems: A global meta-analysis of in situ studies. *J. Hydrol.* **2019**, *576*, 123–136. [CrossRef]
5. Hu, X.; Lei, H. Evapotranspiration partitioning and its interannual variability over a winter wheat-summer maize rotation system in the North China Plain. *Agric. For. Meteorol.* **2021**, *310*, 108635. [CrossRef]
6. Wei, Z.; Lee, X.; Wen, X.; Xiao, W. Evapotranspiration partitioning for three agro-ecosystems with contrasting moisture conditions: A comparison of an isotope method and a two-source model calculation. *Agric. For. Meteorol.* **2018**, *252*, 296–310. [CrossRef]
7. Jha, P.K.; Kumar, S.N.; Ines, A.V.M. Responses of soybean to water stress and supplemental irrigation in upper Indo-Gangetic plain: Field experiment and modeling approach. *Field Crop. Res.* **2018**, *219*, 76–86. [CrossRef]
8. Xu, Z.; Zhu, Z.; Liu, S.; Song, L.; Wang, X.; Zhou, S.; Yang, X.; Xu, T. Evapotranspiration partitioning for multiple ecosystems within a dryland watershed: Seasonal variations and controlling factors. *J. Hydrol.* **2021**, *598*, 126483. [CrossRef]
9. Seck, P.A.; Diagne, A.; Mohanty, S.; Wopereis, M.C.S. Crops that feed the world7: Rice. *Food Secur.* **2012**, *4*, 7–24. [CrossRef]
10. Ray, D.K.; Ramankutty, N.D.; Mueller, P.C.; West, W.J.; Foley, J.A. Recent patterns of crop yield growth and stagnation. *Nat. Commun.* **2012**, *3*, 1293. [CrossRef]
11. Tuong, P.; Bouman, B.A.M.; Mortimer, M. More Rice, Less Water-Integrated Approaches for Increasing Water Productivity in Irrigated Rice-Based Systems in Asia. *Plant Prod. Sci.* **2005**, *8*, 231–241.
12. Allen, R.G.; Pereira, L.S.; Raes, D.; Smith, M. Crop Evapotranspiration Guidelines for Computing Crop Water Requirements. *FAO Irrig. Drain. Pap.* **1998**, *300*, D05109.

13. Jiang, X.; Kang, S.; Tong, L.; Li, F.; Li, D.; Ding, R.; Qiu, R. Crop coefficient and evapotranspiration of grain maize modified by planting density in an arid region of northwest China. *Agric. Water Manag.* **2014**, *142*, 135–143. [CrossRef]
14. Xu, L.; Zhan, X.; Yu, T.; Nie, L.; Huang, J.; Cui, K.; Wang, F.; Li, Y.; Peng, S. Yield performance of direct-seeded, double-season rice using varieties with short growth durations in central China. *Field Crop. Res.* **2018**, *227*, 49–55. [CrossRef]
15. Zhao, Y.; Mao, X.M.; Shukla, M.K.; Tian, F.; Hou, M.J.; Zhang, T.; Li, S.E. How does film mulching modify available energy, evapotranspiration, and crop coefficient during the seed-maize growing season in northwest China? *Agric. Water Manag.* **2021**, *245*, 106666. [CrossRef]
16. Facchi, A.; Gharsallah, O.; Corbari, C.; Masseroni, D.; Mancini, M.; Gandolfi, C. Determination of maize crop coefficients in humid climate regime using the eddy covariance technique. *Agric. Water Manag.* **2013**, *130*, 131–141. [CrossRef]
17. Guo, H.; Li, S.E.; Kang, S.Z.; Du, T.S.; Tong, L.; Hao, X.M.; Ding, R.S. Crop coefficient for spring maize under plastic mulch based on 12-year eddy covariance observation in the arid region of Northwest China. *J. Hydrol.* **2020**, *588*, 125108. [CrossRef]
18. Mao, Z.; Dong, B.; Pereira, L.S. Assessment and water saving issues for Ningxia paddies, upper Yellow River Basin. *Paddy Water Environ.* **2004**, *2*, 99–110. [CrossRef]
19. Choudhury, B.U.; Singh, A.K. Estimation of crop coefficient of irrigated transplanted puddled rice by field scale water balance in the semi-arid Indo-gangetic Plains, India. *Agric. Water Manag.* **2016**, *176*, 142–150. [CrossRef]
20. Lv, Y.P.; Xu, J.Z.; Yang, S.H.; Liu, X.Y.; Zhang, J.G.; Wang, Y.J. Inter-seasonal and cross-treatment variability in single-crop coefficients for rice evapotranspiration estimation and their validation under drying-wetting cycle conditions. *Agric. Water Manag.* **2018**, *196*, 154–161. [CrossRef]
21. Alberto, M.C.R.; Wassmann, R.; Hirano, T.; Miyata, A.; Hatano, R.; Kumar, A.; Padre, A.; Amante, M. Comparisons of energy balance and evapotranspiration between flooded and aerobic rice fields in the Philippines. *Agric. Water Manag.* **2011**, *98*, 1417–1430. [CrossRef]
22. Kumari, A.; Upadhyaya, A.; Jeet, P.; AI-Ansari, N.; Rajput, J.; Sundaram, P.K.; Saurabh, K.; Prakash, V.; Singh, A.K.; Raman, R.K.; et al. Estimation of actual evapotranspiration and crop coefficient of transplanted puddled rice using a modified non-weighing paddy lysimeter. *Agronomy* **2022**, *12*, 2850. [CrossRef]
23. Chatterjee, S.; Stoy, P.C.; Debnath, M.; Nayak, A.K.; Swain, C.K.; Tripathi, R.; Chatterjee, D.; Mahapatra, S.S.; Talib, A.; Pathak, H. Actual evapotranspiration and crop coefficients for tropical lowland rice (*Oryza sativa* L.) in eastern India. *Thero. Appl. Climatol.* **2021**, *146*, 155–171. [CrossRef]
24. Alberto, M.C.R.; Quilty, J.R.; Buresh, R.J.; Wassmann, R.; Haidar, S.; Correa, T.Q., Jr.; Sandro, J.M. Actual evapotranspiration and dual crop coefficients for dry-seeded rice and hybrid maize grown with overhead sprinkler irrigation. *Agric. Water Manag.* **2014**, *136*, 1–12. [CrossRef]
25. Vories, E.D.; Stevens, W.E.; Tacker, P.L.; Griffin, T.W.; Counce, P.A. Rice production with center pivot irrigation. *Appl. Eng. Agric.* **2013**, *29*, 51–60. [CrossRef]
26. Liu, B.; Cui, Y.; Tan, J.; Luo, Y.; Xiang, Z. CO_2 fluxes over two paddy fields with different management practices in Southern China. *Agric. For. Meteorol.* **2021**, *310*, 108650. [CrossRef]
27. Linder, S.; Xue, W.; Nay-Htoon, B.; Choi, J.; Ege, Y.; Lichtenwald, N.; Fischer, F.; Ko, J.H.; Tenhunen, J.; Otieno, D. Canopy scale CO_2 exchange and productivity of transplanted paddy and direct seeded rainfed rice production systems in S. Korea. *Agric. For. Meteorol.* **2016**, *228–229*, 229–238. [CrossRef]
28. Xu, L.; Yuan, S.; Wang, X.; Chen, Z.; Li, X.; Cao, J.; Wang, F.; Huang, J.; Peng, S. Comparison of yield performance between direct-seeded and transplanted double-season rice using ultrashort-duration varieties in central China. *Crop J.* **2022**, *10*, 515–523. [CrossRef]
29. Linquist, B.; Snyder, R.; Anderson, F.; Espino, L.; Inglese, G.; Marras, S.; Moratiel, R.; Mutters, R.; Nicolosi, P.; Rejmanek, H.; et al. Water balances and evapotranspiration in water- and dry seeded rice systems. *Irrig. Sci.* **2015**, *33*, 375–385. [CrossRef]
30. Pereira, L.S.; Paredes, P.; Hunsaker, D.J.; López-Urrea, R.; Shad, Z.M. Standard single and basal crop coefficients for field crops. Updates and advances to the FAO56 crop water requirements method. *Agric. Water Manag.* **2021**, *243*, 106466. [CrossRef]
31. Jiao, L.; Ding, R.; Kang, S.; Du, T.; Tong, L.; Li, S. A comparison of energy partitioning and evapotranspiration over closed maize and sparse grapevine canopies in northwest China. *Agric. Water Manag.* **2018**, *203*, 251–260. [CrossRef]
32. Hu, X.; Chen, M.; Liu, D.; Li, D.; Jin, L.; Liu, S.; Cui, Y.; Dong, B.; Khan, S.; Luo, Y. Reference evapotranspiration change in Heilongjiang Province, China from 1951 to 2018: The role of climate change and rice area expansion. *Agric. Water Manag.* **2021**, *253*, 106912. [CrossRef]
33. Liu, B.; Cui, Y.; Shi, Y.; Cai, X.; Luo, Y.; Zhang, L. Comparison of evapotranspiration measurements between eddy covariance and lysimeters in paddy fields under alternate wetting and drying irrigation. *Paddy Water Environ.* **2019**, *17*, 725–739. [CrossRef]
34. Liu, B.; Cui, Y.; Luo, Y.; Shi, Y.; Liu, M.; Liu, F. Energy partitioning and evapotranspiration over a rotated paddy field in Southern China. *Agric. For. Meteorol.* **2019**, *276–277*, 107626. [CrossRef]
35. LI-COR Biosciences. *EddyPro 5.0: Help and User's Guide*; LI-COR Biosciences: Lincoln, NE, USA, 2013.
36. Webb, E.K.; Pearman, G.I.; Leuning, R. Correction of flux measurements for density effects due to heat and water vapour transfer. *Quart. J. R. Met. Soc.* **1980**, *106*, 85–100. [CrossRef]
37. Fratini, G.; Ibrom, A.; Arriga, N.; Burba, G.; Papale, D. Relative humidity effects on water vapour fluxes measured with closed-path eddy-covariance systems with short sampling lines. *Agric. For. Meteorol.* **2012**, *165*, 53–63. [CrossRef]

38. Wutzler, T.; Lucas-Moffat, A.; Migliavacca, M.; Knauer, J.; Sickel, K.; Šigut, L.; Menzer, O.; Reichstein, M. Basic and extensible post-processing of eddy covariance flux data with REddyProc. *Biogeoscience* **2018**, *15*, 5015–5030. [CrossRef]
39. Falge, E.; Baldocchi, D.; Olson, R.; Anthoni, P.; Aubinet, M.; Bernhofer, C.; Burba, G.; Ceulemans, R.; Clement, R.; Dolman, H.; et al. Gap filling strategies for defensible annual sums of net ecosystem exchange. *Agric. For. Meteorol.* **2001**, *107*, 43–69. [CrossRef]
40. Schmidt, M.; Reichenau, T.G.; Fiener, P.; Schneider, K. The carbon budget of a winter wheat field: An eddy covariance analysis of seasonal and inter-annual variability. *Agric. For. Meteorol.* **2012**, *165*, 114–126. [CrossRef]
41. Zhou, S.; Yu, B.; Zhang, Y.; Huang, Y.; Wang, G. Partitioning evapotranspiration based on the concept of underlying water use efficiency. *Water Resour. Res.* **2016**, *52*, 1160–1175. [CrossRef]
42. Zhou, S.; Yu, B.; Zhang, Y.; Huang, Y.; Wang, G. Water use efficiency and evapotranspiration partitioning for three typical ecosystems in the Heihe River Basin, northwestern China. *Agirc. For. Meteorol.* **2018**, *253–254*, 261–273. [CrossRef]
43. Chen, Y.; Ding, Z.; Yu, P.; Yang, H.; Song, L.; Fan, L.; Han, X.; Ma, M.; Tang, X. Quantifying the variability in water use efficiency from the canopy to ecosystem scale across main croplands. *Agric. Water Manag.* **2022**, *262*, 107427. [CrossRef]
44. Jiang, S.; Liang, C.; Cui, N.; Zhao, L.; Liu, C.; Feng, Y.; Hu, X.; Gong, D.; Zou, Q. Water use efficiency and its drivers in four typical agroecosystems based on flux tower measurements. *Agric. For. Meteorol.* **2020**, *295*, 108200. [CrossRef]
45. Wang, Y.; Cai, H.; Yu, L.; Peng, X.; Xu, J.; Wang, X. Evapotranspiration partitioning and crop coefficient of maize in dry semi-humid climate regime. *Agric. Water Manag.* **2020**, *236*, 106164. [CrossRef]
46. Liu, B.; Wang, W.; Cui, Y.; Xu, T. Partitioning evapotranspiration using the water-carbon flux coupling in a paddy field in the Middle and Lower Reaches of the Yangtze River in China. *Trans. CSAE* **2021**, *37*, 94–101. (In Chinese with English abstract)
47. Jiang, S.; Liang, C.; Cui, N.; Zhao, L.; Du, T.; Hu, X.; Feng, Y.; Guan, J.; Feng, Y. Impacts of climatic variables on reference evapotranspiration during growing season in Southwest China. *Agric. Water Manag.* **2019**, *216*, 365–378. [CrossRef]
48. Reavis, C.W.; Suvočarev, K.; Reba, M.L.; Runkle, B.R.K. Impacts of alternate wetting and drying and delayed flood rice irrigation on growing season evapotranspiration. *J. Hydrol.* **2021**, *596*, 126080. [CrossRef]
49. Monteith, J.L.; Unsworth, M.H. *Principles of Environmental Physics*; Academic Press: New York, NY, USA, 2008.
50. Wilson, K.; Goldstein, A.; Falge, E.; Aubinet, M.; Baldocchi, D.; Berbigier, P.; Bernhofer, C.; Ceulemans, R.; Dolman, H.; Field, C.; et al. Energy balance closure at FLUXNET sites. *Agric. For. Meteorol.* **2002**, *113*, 223–243. [CrossRef]
51. Li, Z.Q.; Yu, G.R.; Wen, X.F.; Zhang, L.M.; Ren, C.Y.; Fu, Y.L. Energy balance closure at ChinaFLUX sites. *Sci. China Ser. D-Earth Sci.* **2005**, *48* (Suppl. I), 51–62.
52. Wohlfahrt, G.; Haslwanter, A.; Hörtnagl, L.; Jasoni, R.L.; Fenstermaker, L.F.; Arnone III, J.A.; Hammerle, A. On the consequences of the energy imbalance for calculating surface conductance to water vapour. *Agric. For. Meteorol.* **2009**, *149*, 1556–1559. [CrossRef]
53. Farooq, M.; Siddique, K.H.M.; Rehman, H.; Aziz, T.; Lee, D.J.; Wahid, A. Rice direct seeding: Experiences, challenges and opportunities. *Soil Till. Res.* **2011**, *111*, 87–98. [CrossRef]
54. Tuong, T.P.; Bouman, B.A.M. *Rice Production in Water-Scarce Environments*; International Water Management Institute: Colombo, Sri Lanka, 2003.
55. Chauhan, B.S.; Opeña, J. Effect of tillage systems and herbicides on weed emergence, weed growth, and grain yield in dry-seeded rice systems. *Field Crop. Res.* **2012**, *137*, 56–69. [CrossRef]
56. Lahue, G.T.; Linquist, B.A. The contribution of percolation to water balances in water-seeded rice systems. *Agric. Water Manag.* **2021**, *243*, 106445. [CrossRef]
57. Sharma, P.K.; Bhushan, L.; Ladha, J.K.; Naresh, R.K.; Gupta, R.K.; Balasubramanian, B.V.; Bouman, B.A.M. Crop–water relations in rice–wheat cropping under different tillage systems and water management practices in a marginally sodic medium textured soil. In *Water-Wise Rice Production*; Bouman, B.A.M., Hengsdijk, H., Hardy, B., Bihdraban, B., Toung, T.P., Ladha, J.K., Eds.; International Rice Research Institute: Los Baños, Philippines, 2002; pp. 223–235.
58. Singh, A.K.; Choudhury, B.U.; Bouman, B.A.M. Effects of rice establishment methods on crop performance, water use and mineral nitrogen. In *Water-Wise Rice Production*; Bouman, B.A.M., Hengsdijk, H., Hardy, B., Bihdraban, B., Toung, T.P., Ladha, J.K., Eds.; International Rice Research Institute: Los Baños, Philippines, 2002; pp. 237–246.
59. Kumar, S.; Narjary, B.; Kumar, K.; Jat, H.S.; Kamara, S.K.; Yadav, R.K. Developing soil matric potential based irrigation strategies of direct seeded rice for improving yield and water productivity. *Agric. Water Manag.* **2019**, *215*, 8–15. [CrossRef]
60. Liu, H.; Hussain, S.; Zheng, M.; Peng, S.; Huang, J.; Cui, K.; Nie, L. Dry direct-seeded rice as an alternative to transplanted-flooded rice in Central China. *Agron. Sustain. Dev.* **2015**, *35*, 285–294. [CrossRef]
61. Tan, X.; Shao, D.; Liu, H.; Yang, F.; Xiao, C.; Yang, H. Effects of alternate wetting and drying irrigation on percolation and nitrogen leaching in paddy fields. *Paddy Water Environ.* **2013**, *11*, 381–395. [CrossRef]
62. Xu, B.; Shao, D.; Fang, L.; Yang, X.; Chen, S.; Gu, W. Modelling percolation and lateral seepage in a paddy field-bund landscape with a shallow groundwater table. *Agric. Water Manag.* **2019**, *214*, 87–96. [CrossRef]
63. Wu, D.; Cui, Y.; Luo, Y. Irrigation efficiency and water-saving potential considering reuse of return flow. *Agric. Water Manag.* **2019**, *221*, 519–527. [CrossRef]
64. Wu, D.; Cui, Y.; Wang, Y.; Chen, M.; Luo, Y.; Zhang, L. Reuse of return flows and its scale effect in irrigation systems based on modified SWAT model. *Agric. Water Manag.* **2019**, *213*, 280–288. [CrossRef]
65. Van Oort, P.A.J.; Dingkuhn, M. Feet in the water and hands on the keyboard: A critical retrospective of crop modelling at Africa Rice. *Field Crop. Res.* **2021**, *263*, 108074. [CrossRef]

66. Li, H.; Guo, H.; Helbig, M.; Dai, S.; Zhang, M.; Zhao, M.; Peng, C.; Xiao, X.; Zhao, B. Does direct-seeded rice decrease ecosystem-scale methane emissions?—A case study from a rice paddy in southeast China. *Agric. For. Meteorol.* **2019**, *272–273*, 118–127. [CrossRef]
67. Wang, Y.; Zhou, L.; Jia, Q.; Yu, W. Water use efficiency of a rice paddy field in Liaohe Delta, Northeast China. *Agric. Water Manag.* **2017**, *187*, 222–231. [CrossRef]
68. Diaz, M.B.; Roberti, D.R.; Carneiro, J.V.; Souza, V.A.; Moraes, O.L.L. Dynamics of the superficial fluxes over a flooded rice paddy in southern Brazil. *Agric. For. Meteorol.* **2019**, *276–277*, 107650. [CrossRef]
69. Vu, S.H.; Watanabe, H.; Takagi, K. Application of FAO-56 for evaluating evapotranspiration in simulation of pollutant runoff from paddy rice field in Japan. *Agric. Water Manag.* **2005**, *76*, 195–210. [CrossRef]
70. Kadiyala, M.D.M.; Mylavarapu, R.S.; Li, Y.C.; Reddy, G.B.; Reddy, M.D. Impact of aerobic rice cultivation on growth, yield, and water productivity of rice-maize rotation in semiarid tropics. *Agron. J.* **2012**, *104*, 1757–1765. [CrossRef]
71. Hatiye, S.D.; HariPrasad, K.S.; Ojha, C.S.P.; Kaushika, G.S.; Adeloye, A.J. Evaluating irrigation scheduling efficiency of paddy rice and berseem fodder crops in sandy loam soil. *Irrig. Drain. Syst. Eng.* **2015**, *4*, 147.
72. Qiu, R.; Li, L.; Liu, C.; Wang, Z.; Zhang, B.; Liu, Z. Evapotranspiration estimation using a modified crop coefficient model in a rotated rice-winter wheat system. *Agric. Water Manag.* **2022**, *264*, 107501. [CrossRef]
73. Pereira, L.S.; Paredes, P.; Melton, F.; Johnson, L.; Mota, M.; Wang, T. Prediction of crop coefficients from fraction of ground cover and height: Practical application to vegetable, field and Fruit crops with focus on parameterization. *Agric. Water Manag.* **2021**, *252*, 106663. [CrossRef]
74. Choudhury, B.U.; Singh, A.K.; Pradhan, S. Estimation of crop coefficients of dry-seeded irrigated rice–wheat rotation on raised beds by field water balance method in the Indo-Gangetic plains, India. *Agric. Water Manag.* **2013**, *123*, 20–31. [CrossRef]
75. Montazar, A.; Rejmanek, H.; Tindula, G.; Little, C.; Shapland, T.; Anderson, F.; Inglese, G.; Mutters, R.; Linquist, B.; Greer, C.A.; et al. Crop Coefficient Curve for Paddy Rice from Residual Energy Balance Calculations. *J. Irrig. Drain. Eng.* **2017**, *143*, 04016076. [CrossRef]
76. Allen, R.G.; Pereira, L.S. Estimating crop coefficients from fraction of ground cover and height. *Irri. Sci.* **2009**, *28*, 17–34. [CrossRef]
77. Qiu, R.; Song, J.; Du, T.; Kang, S.; Tong, L.; Chen, R.; Wu, L. Response of evapotranspiration and yield to planting density of solar greenhouse grown tomato in northwest China. *Agric. Water Manag.* **2013**, *130*, 44–51. [CrossRef]
78. Chen, Z.; Sun, S.; Zhu, Z.; Jiang, H.; Zhang, X. Assessing the effects of plant density and plastic film mulch on maize evaporation and transpiration using dual crop coefficient approach. *Agric. Water Manag.* **2019**, *225*, 105765. [CrossRef]
79. Ding, R.; Tong, L.; Li, F.; Zhang, Y.; Hao, X.; Kang, S. Variations of crop coefficient and its influencing factors in an arid advective cropland of northwest China. *Hydrol. Process.* **2015**, *29*, 239–249. [CrossRef]